Journal of
Ceramic Science
and Technology

J. Ceram. Sci. Tech., **06** [01] 17-24 (2015)
DOI: 10.4416/JCST2014-00034
available online at: http://www.ceramic-science.com

Evolution of the Fibre-Matrix Interactions in Basalt-Fibre-Reinforced Geopolymer-Matrix Composites after Heating

M. Welter*[1], M. Schmücker[2], K.J.D. MacKenzie[1]

[1]MacDiarmid Institute of Advanced Materials and Nanotechnology, School of Chemical and Physical Sciences, Victoria University of Wellington, New Zealand
[2]German Aerospace Center, Institute of Materials Research, Cologne, Germany
received August 15, 2014; received in revised form September 12, 2014; accepted October 1, 2014

Abstract

The evolution of fibre-matrix interactions in basalt-fibre-reinforced geopolymer matrix composites after heating to 600, 800 and 1000 °C was investigated by means of SEM, EDS and XRD analyses. The basalt fibres showed no significant interfacial interaction up to 600 °C. The appearance of the fracture surfaces also remained largely unchanged. At higher temperatures, crystallisation reactions within the fibres and the Na-geopolymer matrix, respectively, could be observed along with an increasing embrittlement of the composite. Softening of the fibres and the development of several distinct reaction zones within the fibres was clearly evident after heating to 800 °C and 1000 °C. The formation of an iron-rich outer reaction zone within the fibre was observed above 800 °C. The interaction between fibre and matrix resulted in the formation of a crystalline albite phase after heating to 1000 °C. It is suggested that basalt fibres have great potential as reinforcements for the development of cost-efficient geopolymer-matrix composites and may be used for applications up to 600 °C.

Keywords: Geopolymer-matrix composites, fibre-matrix interaction, interface, basalt fibre

I. Introduction

Recent advances in technological development have seen an ever-growing commercial relevance of fibre-reinforced composite materials in all fields of applications. In particular, polymer-matrix composites (PMCs) have found widespread use due to their excellent properties at room temperature and their comparatively easy and cost-effective fabrication methods at moderate temperatures. However, the main drawback of PMCs is the limited temperature stability of the organic matrices, typically restricting their use to operating temperatures below 200 °C. Thus, metal- or ceramic-based materials must be used for applications at higher temperatures. Ceramics generally exhibit very desirable properties such as relatively low density, high strength and stiffness, chemical stability and superior high-temperature properties. However, the inherently brittle nature of ceramic materials is a major limitation for their widespread use in structural and engineering applications. This problem can be largely overcome by the incorporation of inorganic fibres to increase the toughness of the matrix, introducing a quasi-ductile, graceful failure behaviour. Despite extensive research efforts over the past decades, however, fibre-reinforced ceramic matrix composites (CMCs) have only recently come to a point of actual commercial relevance. Nevertheless, the much higher overall costs of CMCs due to more complex processing requirements, higher material costs and much higher manufacturing temperatures are still a significant limitation for their widespread use. Whereas the high costs may be justified in some highly demanding applications, their use for less demanding applications at temperatures below around 600 – 800 °C becomes increasingly uneconomical. This essentially only leaves metal-based materials for applications in the temperature range from about 200 – 800 °C. However, several factors such as higher density, insufficient corrosion resistance, electrical conductivity or costs may make the use of metals unfavourable. Thus, the development of new inorganic, non-metal materials that can essentially combine the advantages of both CMCs and PMCs, i.e. high strength, low density and reasonably high temperature stability, in a cost-effective way for applications in this mid-temperature range would be highly desirable.

In this regard, inorganic aluminosilicate polymers, also called geopolymers, may offer an alternative to common polymer and ceramic matrix materials. The attraction of geopolymers as matrix materials for composites arises from the combination of properties, most noteworthy their temperature stability up to 800 – 1000 °C, and the relatively easy processing and fabrication methods similar to those of PMCs. These aspects essentially combine two of the main advantages of polymer and ceramic composites, respectively. Therefore, geopolymer-matrix composites (GMCs) possess significant potential as economical alternatives to conventional CMCs for applications in a mid-temperature range up to ~ 800 °C, effectively bridging the gap between existing PMC and CMC materials.

* Corresponding author: michael.welter@dlr.de

A number of different fibre-reinforced geopolymer-matrix composites using a variety of short and continuous fibres such as carbon, silicon carbide (SiC), alumina, aluminosilicate, basalt and glass fibres have been investigated since geopolymer composites were first proposed in the 1980s [1–29]. In particular for continuous fibre-reinforced composites, the main contributor to the overall cost of the composites are the fibre costs. Whereas CMCs typically demand the use of advanced inorganic fibres such as SiC and alumina owing to their high processing temperatures, the low-temperature processing of geopolymers (typically < 100 °C) also allows the use of cheaper and less advanced fibres. Even the use of (synthetic) organic and natural fibres may be feasible for certain applications and a number of studies have been carried out on this subject [2, 30–36]. However, the limited temperature stability of these fibres militates against their application at elevated temperatures.

One of the most inexpensive and commonly used inorganic fibre types in PMCs are E-glass fibres. However, the highly alkaline conditions during the geopolymer processing restrict their usability in GMCs due to the limited alkali stability of E-glass fibres resulting in significantly degraded fibres in the composite. The alkali stability of the glass fibres depends on the overall glass composition, mainly the alkali, SiO_2 and B_2O_3 contents. The detrimental effect of a highly alkaline geopolymer binder on the stability of an aluminosilicate fibre with high B_2O_3 content was shown by Foerster [2].

An alternative to common glass fibres are basalt fibres. Although very similar to glass fibres, the combination of better alkali resistance and better mechanical properties compared to E-glass fibres and the significantly lower cost compared to carbon or alumina fibres make basalt fibres a very interesting candidate for the fabrication of cost-effective composites.

The use of basalt fibres as reinforcements for GMCs, mostly in form of short fibres, has been reported by several authors [15, 22–27]. These studies mostly address the mechanical properties of the respective composites. However, the microstructural interaction between fibre and matrix in GMCs, in particular the evolution of the fibre-matrix interactions of basalt-fibre GMCs with temperature, has so far not been investigated in any detail. Therefore, the present study investigates the microstructural evolution of the fibre-matrix interactions in unidirectional basalt-fibre-reinforced GMCs as a function of heat treatment temperature up to 1000 °C. The results give an indication up to which temperature the use of basalt fibres as reinforcements for geopolymers may be feasible.

II. Experimental

The geopolymer matrix (M1) with a calculated composition of SiO_2/Al_2O_3 = 3.0, Na_2O/SiO_2 = 3.6 and H_2O/Na_2O = 10.1 was prepared from a dehydroxylated halloysite and a pre-dissolved alkali activator solution. The halloysite (Imerys Tableware, NZCC Halloysite Premium, Grade: Ultrafine – H; d_{50} ~ 0.3 µm) was dehydroxylated at 600 °C overnight. The chemical composition of the dehydroxylated halloysite is given in Table 1. The main phase of the dehydroxylated halloysite was x-ray amorphous with minor crystalline phases of quartz and cristobalite. The alkali activator solution was made by mixing a 12.5M NaOH solution with a commercially available sodium silicate solution (Orica Chemnet, Grade D, SiO_2/Na_2O ~ 2, 29.4 wt% SiO_2) in a 3:2 weight ratio. The dehydroxylated halloysite was slowly added to the alkali solution under constant stirring at about 250 rpm. The mixture was further homogenised for about five minutes before use.

The basalt fibres used in this study had a diameter ~ 13 µm and were used in form of continuous fibre tows (R&G Faserverbundwerkstoffe, 2400 tex). The chemical composition of the basalt fibres is shown in Table 2. The fibres were used as-received, i.e. the fibre sizing was not removed prior to composite fabrication, since preliminary investigations revealed that the fibre sizing was removed under the highly alkaline conditions. Unidirectional fibre-reinforced geopolymer-matrix composite bars with a size of approximately 3 x 10 x 120 mm (h x w x l) were fabricated by the hand lay-up of ten impregnated fibre tapes in plastic moulds. To prepare the fibre tapes, the continuous fibre tow was first stretched over a large-diameter glass tube in a small sideward motion to loosen the individual fibres and to improve fibre alignment. The continuous tow was then fixed with adhesive tape at lengths of around 150 mm and cut across the taped areas to produce individual fibre tapes. Each fibre tape was impregnated with the geopolymer binder from both sides with a roller. The moulds were sealed and cured in an oven at 40 °C for 48 hours. All specimens were subsequently dried under ambient conditions for a minimum of seven days before further testing and analysis. The fibre volume content was about 30 vol%.

Table 1: Chemical composition of dehydroxylated halloysite.

Oxide	*SiO_2*	*Al_2O_3*	*Fe_2O_3*	*TiO_2*	*CaO*	*MgO*	*K_2O*	*Na_2O*	*P_2O_5*	*LOI*
wt%	56.61	40.96	0.34	0.08	0.01	0.02	0.01	<0.01	0.19	1.43

*LOI = Loss on ignition at 1000 °C for 1 hour

Table 2: Chemical analysis of basalt fibre.

Oxide	*SiO_2*	*Al_2O_3*	*Fe_2O_3*	*TiO_2*	*CaO*	*MgO*	*K_2O*	*Na_2O*	*P_2O_5*
wt%	54.58	17.51	9.80	1.10	8.02	3.91	1.66	2.44	0.19

Cut composite bar pieces of 30 – 40 mm length were heated to 600, 800 and 1000 °C in air and annealed for 60 minutes according to the heating programme shown in Fig. 1. The interfacial reaction was investigated by means of scanning electron microscopy (SEM) and EDS line scan analysis on fractured and polished surfaces using a JEOL JSM 6500F electron microscope. In order to directly compare the change in concentration of the various elements irrespective of their absolute abundance, all line scan profiles presented in this study were normalised with regards to the maximum intensity of each element. All SEM samples were carbon-coated. X-ray powder diffraction analysis (XRD, PANalytical X'Pert PRO MPD, Cu $K\alpha_1$ radiation: $\lambda = 1.5418$ Å) of ground composite specimens was used to identify any crystalline phase formations. The software PANalytical X'Pert HighScore was used for phase analysis.

The chemical stability of the basalt fibres was tested in a preliminary experiment in a concentrated 12.5M NaOH solution for 150 h at 40 °C to identify potential fibre degradation due to alkali attack. The preliminary corrosion test showed no signs of fibre degradation under the highly alkaline conditions, thus indicating the general suitability of basalt fibres for use as reinforcements in geopolymer-matrix composites. Only the removal of the fibre sizing was noted.

III. Results and Discussion

The SEM and EDS analyses of the unheated composite showed no apparent reaction between fibre and matrix. Fig. 2 shows the polished surface of an unheated composite sample and the corresponding EDS line scan profiles of the relevant elements across the interface. It can be seen that most element profiles show a relatively abrupt change of intensity in close proximity to the fibre edge. Only the sodium and potassium profiles displayed a somewhat gentler change of intensity across the fibre-matrix interface. This indicates that some degree of fibre-matrix interaction in form of alkali diffusion occurs at room temperature over time.

The electron microscopic analysis revealed no evidence of the retention of the fibre sizing. It is suspected that the fibre sizing dissolves into the geopolymer matrix due to the high alkalinity in accordance with the observations made in the preliminary fibre corrosion test. Although the dissolution of the fibre sizing did not appear to have any apparent effect on the composite's structure or integrity, further investigations are needed to fully comprehend the role of the fibre sizing and its possible consequences for the properties of the fibre-matrix interface and the matrix itself.

XRD analysis did not indicate the formation of any crystalline phases as a result of fibre-matrix interaction. This is consistent with the observations from the SEM analysis. As can be seen from Fig. 3, the XRD pattern of the basalt-fibre composite is essentially a combination of the diffractograms of the individual components. The quartz and cristobalite peaks arose from unreacted crystalline impurities in the halloysite starting material.

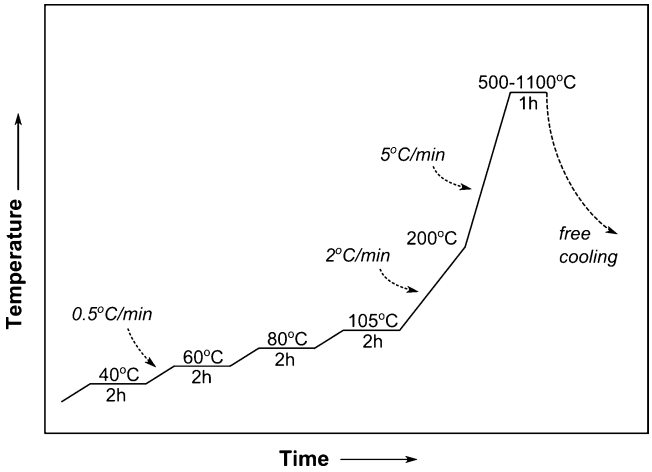

Fig. 1: Schematic of standard heating programme.

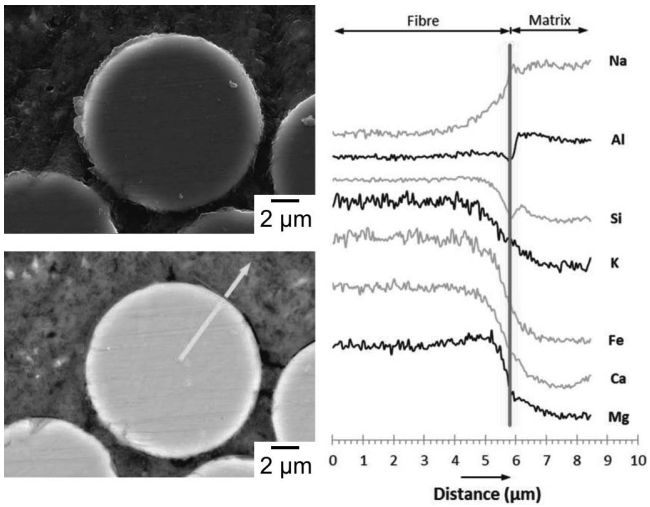

Fig. 2: SEI and BSE-SEM micrographs of polished surface of M1-Basalt composite and corresponding EDS line scan profile across the fibre matrix interface.

The fracture surface of the unheated basalt-fibre composites was characterised by long debonded fibres with considerable matrix fragmentation and some extent of fibre fracture.

The macro- and microscopic appearance and fracture behaviour of the composite sample heated to 600 °C showed only little difference compared to the unheated composite. The heated sample also showed a large number of small matrix cracks perpendicular to the fibre orientation as a result of drying and shrinkage of the matrix. However, no interfacial reaction could be observed. The typical appearance of the fracture surface of the composite sample after heating to 600 °C is shown in Fig. 4(a). Fibres that did not fracture had to be cut. Some small grey-black spots on the sample surface were evidence of incomplete burnout of the fibre sizing. The XRD analysis confirmed that no significant phase changes took place after heating of the basalt-fibre composite sample to 600 °C (see Fig. 3). Only a slight shift of the amorphous hump and a small reduction of the quartz and cristobalite peaks could be observed. This indicates a change in the amorphous geopolymer network structure as well as an increasing dissolution of the crystalline SiO_2 impurities into the matrix with increasing temperature.

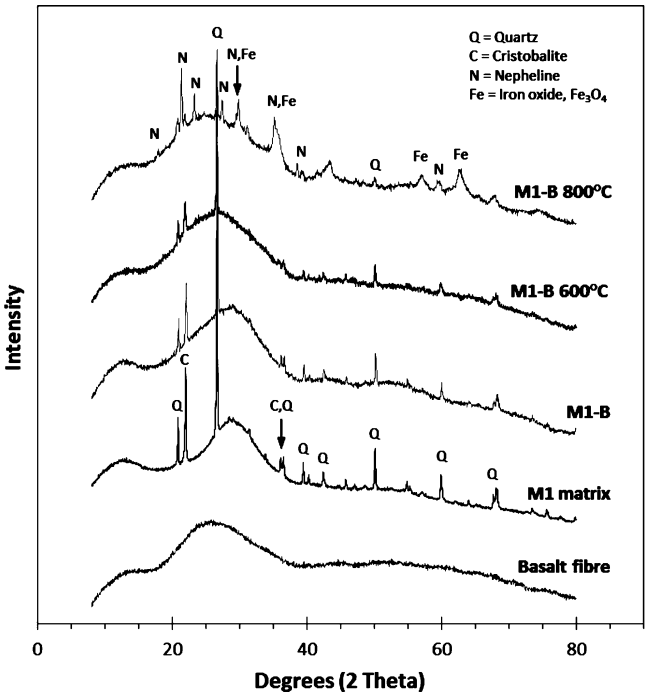

Fig. 3: X-ray diffraction patterns of basalt fibre, M1 matrix and M1-Basalt composite at room temperature and after heating to 600 and 800 °C for 1 h in air.

A colour change of the basalt composite sample from green to black was observed after heating to 800 °C. This was accompanied by microstructural changes in the composite, predominantly within the fibres. Although the basalt fibres appeared unchanged under standard SEM imaging conditions, the formation of a reaction zone along the inner fibre edge of most fibres was revealed in backscattered mode, see Fig. 5. However, the characteristic of this reaction zone was less pronounced for some fibres than for others. Fig. 5(b) shows a typical approximately 2-µm-wide reaction zone, characterised by the formation of nano-crystallites, around the inner fibre edge. The corresponding EDS line scan profile clearly indicates the concentration of iron in the reaction zone but also considerable interdiffusion between the fibre and the matrix, in particular for sodium, potassium and calcium. The magnesium concentration also shows a marked gradient between the fibre centre and the outer fibre reaction zone. Hence, it can be concluded that potassium and calcium ions diffuse from the fibre into the matrix whereas sodium diffuses from the matrix into the fibre. The diffusion of the magnesium seems inverse to the iron diffusion within the fibre.

XRD analysis confirmed the formation of a crystalline iron oxide phase which matched the diffraction pattern of Fe_3O_4 (PDF No. 04 – 013 – 9811) after heating to 800 °C, see Fig. 3. The crystallisation of Fe_3O_4 is consistent with the observed colour change of the composite sample. The XRD analysis also identified another crystalline phase, i.e. nepheline (PDF No. 04 – 012 – 4977). This phase can be attributed to the onset of matrix crystallisation also observed in the unreinforced geopolymer matrix after heating to 800 °C.

The crystallisation reaction within the fibre along with an increased densification of the matrix caused a marked embrittlement of both the fibre and the composite after heating to 800 °C, as can be seen in Fig. 4(b). The fracture surface was characterised by several fracture planes indicating a strong fibre-matrix bond and only minor fibre debonding and pullout. Higher temperature exposure resulted in completely brittle failure behaviour with a single fracture plane (Fig. 4(c)).

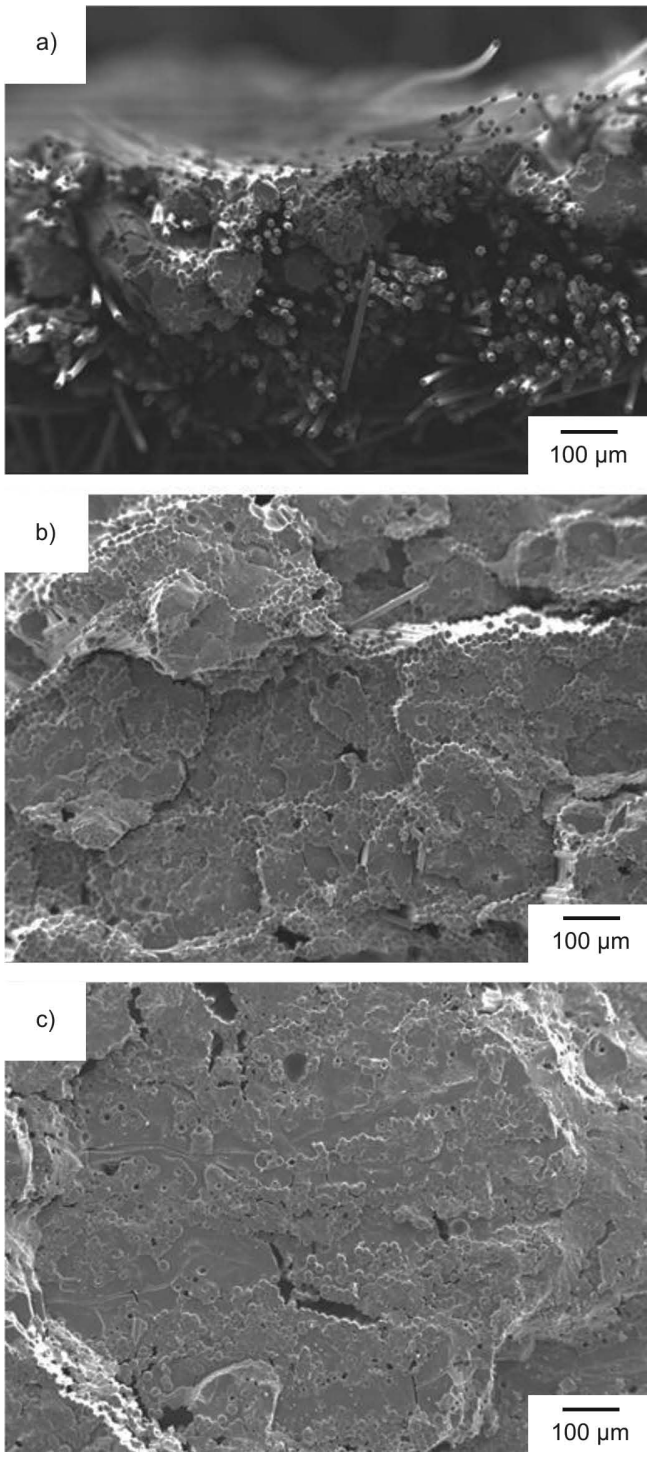

Fig. 4: Fracture surfaces of basalt fibre composites after heating to (a) 600 °C, (b) 800 °C and (c) 1000 °C.

Heating to 1000 °C resulted in another colour change of the composite sample from black to brown-orange. At higher magnification, further crystallisation reactions along with a significant deformation of the fibres were evident, as shown in Fig. 6. In particular in densely packed

fibre areas, the fibre deformation was accompanied by a marked shape accommodation of the surrounding fibres. However, the consolidation of two neighbouring fibres, as can be seen in Fig. 7, was hardly observed to occur. Fig. 6 indicates the formation of at least three distinct reaction zones within the basalt fibres. The formation of an approximately 200-nm-wide outer reaction zone along the inner fibre edge which appeared as a bright line in the backscattered electron micrographs was common to all fibres. Crystallisation was evident in the centre of the fibres. However, Fig. 6(b) clearly shows that the size and shape of crystallites forming in the inner reaction zone varied to considerable degrees. The size of the crystallites in this zone ranged from the low nanometre scale up to around 1 µm. The inner and outer reaction zones were separated by a ~ 2-µm-wide band which forms the intermediate reaction zone. A fine distribution of tiny bright spots was revealed by high-resolution backscattered electron imaging, indicating that this zone was also subject to some form of precipitation or crystallisation reaction. However, in contrast to the inner fibre zone, this zone showed similar appearance in all fibres.

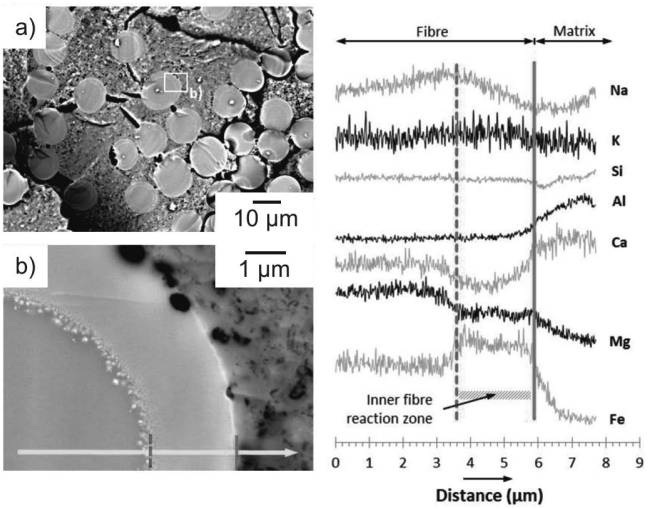

Fig. 5: BSE-SEM images of the fracture surface of M1-Basalt composite after heating to 800 °C for 1 h. EDS line scan analysis indicates the formation of an iron-rich inner fibre reaction zone.

According to the EDS line scan profile in Fig. 6 a significant percentage of the present calcium diffused into the matrix. The sodium, on the other hand, diffused from the matrix into the outer parts of the fibre up to about ~ 4 µm from the fibre edge whereas the potassium content was lower in that area compared to the fibre centre. The behaviour of the iron and magnesium profiles was relatively similar to the one observed at 800 °C, at least for the fibre on the right-hand side of the line scan, indicating a higher concentration of iron around the fibre edges. EDS line scan analysis at higher magnification confirmed a peak concentration of iron in the outermost reaction zone of the fibre, as shown in Fig. 7.

Some variation to the described ion diffusion transport was observed in some areas of the sample, in particular for the alkali and calcium ions. These differences may be attributed in some degree to slight variations in the chemical composition of the individual basalt fibres. However, a pronounced influence of the immediate chemical environment around each fibre also has to be considered. That is, fibres in high fibre density regions may show a somewhat different crystallisation and reaction behaviour from fibres that are surrounded by larger amounts of matrix.

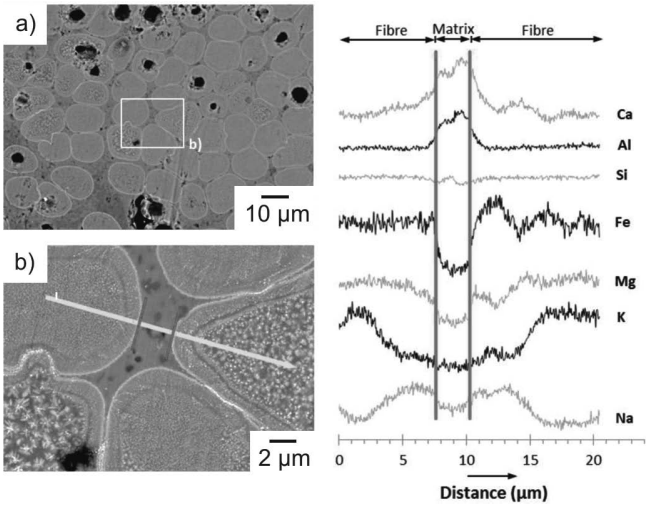

Fig. 6: BSE-SEM images and corresponding EDS line scan profile across the fibre-matrix interface of the polished surface of the M1-Basalt composite after heating to 1000 °C. The micrographs show the marked fibre deformation, shape accommodation and crystallisation within the fibre.

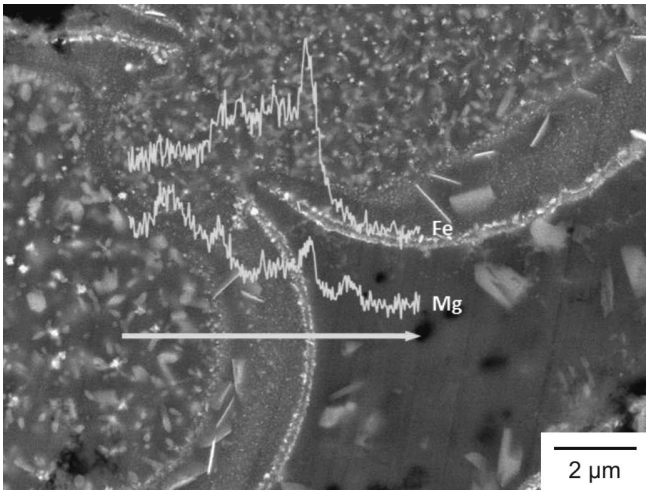

Fig. 7: BSE-SEM image of the fibre-matrix interface of the M1-Basalt composite after heating to 1000 °C at higher magnification with overlay of EDS line scan profile for Fe and Mg.

Since most of the reactions in the heated basalt composites seemed to occur within the fibre, a bundle of loose basalt fibres was heated to 1000 °C in order to compare the reaction in the fibre without any surrounding geopolymer matrix. A micrograph of the cross-section of the fractured fibre bundle is shown in Fig. 8. The image shows that only a very small number of fibres resembled the approximate reaction pattern of the fibres in the composite sample. Although the formation of nano-precipitates especially along the fibre edges was evident at higher magnification for all fibres, the formation of a distinct outer reaction zone similar to the one observed in the composite sample was indicative at best. A slight deformation of the fibre cross-section and the formation of sinter-necks between fibres were also clearly visible.

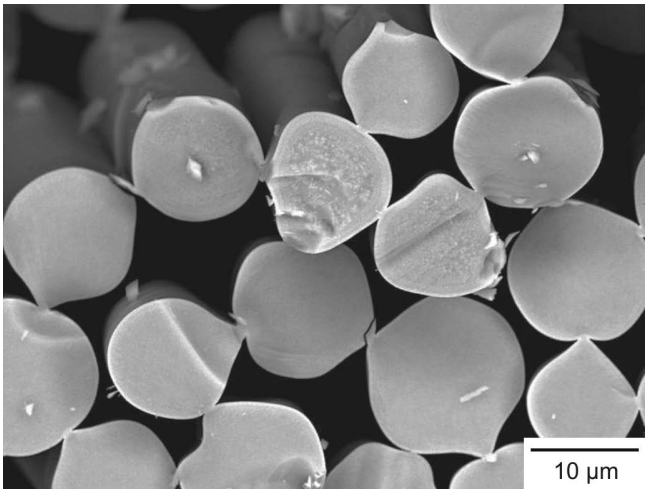

Fig. 8: BSE-SEM image of a fractured basalt fibre bundle after heating to 1000 °C for 1 h.

Fig. 9 shows the XRD diffractograms of the matrix, the fibre and the composite after heating to 1000 °C. The matrix alone showed nearly complete crystallisation with nepheline (PDF No. 04 – 012 – 4977) as the sole crystalline phase. The diffractogram of the basalt fibre only indicated partial crystallisation of the amorphous fibre after heating to 1000 °C. Almost all of the main diffraction peaks could be attributed to some form of Ca-Mg-Al-silicate with the possible incorporation of small amounts of iron (PDF-No. 01 – 076 – 2661 and 01 – 089 – 5691). Although the exact composition could not be determined, this phase appears to be a pyroxene-type solid solution of the respective elements. A form of iron oxide (Fe_2O_3, PDF No. 04 – 011 – 7764) was also detected.

The XRD diffractogram of the heated composite was very complex and was dominated by the nepheline peaks originating from the crystallising matrix. Other phases that could be identified with relative certainty were the afore-mentioned Ca-(Fe)-Mg-Al-silicate phase as well as a new sodium-rich feldspar-type solid solution of albite with some degree of potassium and possibly calcium substitution. The best fit showed a diffraction pattern for a potassium substituted albite ($K_xNa_{1-x}AlSi_3O_8$, x = 0.2, PDF No. 04 – 011 – 6768). The presence of other crystalline phases, in particular various iron oxide compounds and/or a Mg-Fe-Al-O spinel-type phase seem likely but their detection may be concealed by the high intensity of the peaks of the dominant phases.

Although the results of the SEM and EDS analyses on the elemental distribution were somewhat inconclusive, the Ca-(Fe)-Mg-Al-silicate phase as well as an iron oxide phase, both of which are present in the heated fibre alone as well as the composite, are believed to form in the two outer reaction zones. The crystallisation of iron oxide in the fibres and the oxidation of Fe_3O_4, found in the 800 °C sample, to Fe_2O_3 after heating to 1000 °C would explain the observed colour change in the fibres and composite.

The role of calcium in the matrix is not fully understood yet as it does not appear to influence the crystallisation of the matrix into nepheline. The XRD analysis did not indicate the formation of a Ca-containing crystalline phase in the matrix as the detected Ca-(Fe)-Mg-Al-silicate phase is believed to crystallise within the outer fibre region. However, EDS elemental maps (not shown here) suggest that some Ca, Mg and Si-rich phases form in the matrix. Nevertheless, crystallisation may only appear at higher temperatures or longer annealing times. Alternatively, the amount of this phase may be too small to be identified in the diffractogram due to all the other phases present.

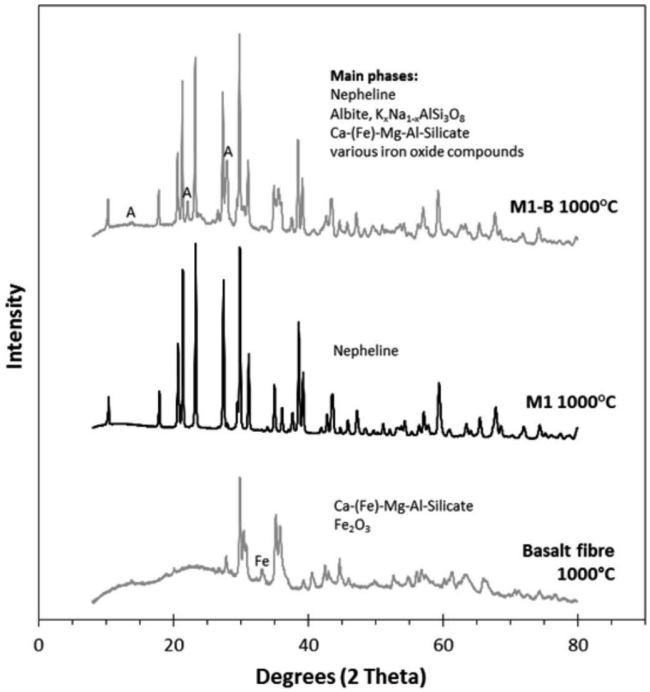

Fig. 9: Comparison of x-ray diffraction patterns of basalt fibre, M1 matrix and M1-Basalt composite after heating to 1000 °C for 1 h. Note: Due to its relative weakness, only the main Fe peak is labelled in the diffractogram of the heated basalt fibre. All other peaks can be attributed to the Ca-(Fe)-Mg-Al-silicate phase and underlying weaker peaks of the iron phase. All peaks in the diffractogram of the heated matrix belong to the nepheline phase. All these phases are also present in the composite. The only new and clearly identifiable phase in the basalt composite was albite. For reasons of clarity, only the main peaks of the albite phase are labelled.

Since the formation of albite was only observed in the composite, it can be concluded that this phase is a product of fibre-matrix interaction facilitated by the interdiffusion of the alkali atoms. The crystallisation of the albite phase is expected to occur most likely in the inner and/or intermediate reaction zone within the fibre. This interaction clearly indicates the significant influence that the presence and chemical nature of the matrix has on the degree of crystallisation and phase formation in the basalt fibres and the composite, respectively. Whereas heating of the basalt fibres alone to 1000 °C indicated some degree of sintering and softening of the fibres, the presence of the highly alkaline matrix amplified these processes considerably. By diffusing into the fibres, the sodium is believed to act like a flux, causing a significant decrease of the softening temperature and at least partial melting of the basalt fibre due the formation of eutectic mixtures. The lower viscosity facilitates easier diffusion transport and reinforces the crystallisation reactions that occur in the fibre. Thus, the fibres essentially act in a similar way as the glassy phase in a classic liquid phase sintering process.

The early softening of the fibres in the composite is also evident from the pore diffusion. With increasing densification of the matrix the accumulation of pores along the fibre-matrix interface and their subsequent diffusion into the fibres was observed at temperatures above 600 °C. The accumulation of small pores around the fibre edges that are starting to penetrate the fibres was clearly evident in the 800 °C sample as can be seen in Fig. 5. With increasing temperature and time the smaller pores continued to diffuse into the centre of the fibres combining into single larger pores inside the fibres as shown in Fig. 6.

IV. Conclusions

The basalt fibre showed no significant degradation or microstructural interaction with the geopolymer matrix up to 600 °C. In combination with their good mechanical properties ($\sigma_{flex,\ max}$ = 194 MPa for the unheated composite [37]) and comparatively low fibre cost, this makes basalt fibre a great alternative as reinforcement for the fabrication of cost-efficient geopolymer-matrix composites. However, increasing crystallisation and melting of the fibre occurred at higher temperatures, resulting in an increasingly brittle failure of the fibre and the composite, respectively. A number of different diffusion processes within the fibre itself and between the fibre and the matrix could be observed. Most notably, the iron in the basalt fibre started to diffuse towards the fibre edges above 600 °C resulting in the formation of a ~2-µm-wide reaction zone, characterised by the formation of nano-sized Fe_3O_4 crystallites, around the inner fibre edge after heating to 800 °C. Other main diffusion processes that were evident were the diffusion of sodium from the matrix into the outer area of the fibre as well as the diffusion of calcium from the fibre into the matrix. Comparison between the heated fibres alone and the heated composite showed that the presence and chemical nature of the matrix had a strong influence on the degree of crystallisation and phase formation in the basalt fibres and the composite, respectively. The various processes resulted in the formation of at least three distinct reaction zones within the basalt fibre after heating to 1000 °C. A direct consequence of the fibre-matrix interaction after heating to 1000 °C was the formation of albite which is believed to form within the fibre.

This study indicates that basalt fibres have great potential as reinforcements for the development of cost-effective GMCs for applications up to 600 °C. Nonetheless, further investigations of the high-temperature mechanical properties of these composites are necessary to validate these results.

Acknowledgements

This work was funded by the MacDiarmid Institute of Advanced Materials and Nanotechnology.

References

1 Davidovits, J.: Geopolymer chemistry and applications, Institut Géopolymère, Saint-Quentin, 2008.

2 Foerster, S.C.: Alkali-activated aluminosilicate composites, (in German), PhD Thesis, ETH Zürich, Switzerland, (1994).

3 Foerster S.C., Graule, T., Gauckler, L.J.: Strength and toughness of reinforced chemically bonded ceramics, In: Cement technology, Ed. Gartner, E.M., Uchikawa, U., *Ceram. Trans.*, **40**, 247 – 256, (1994).

4 Foerster S.C., Graule, T., Gauckler, L.J.: Thermal and mechanical properties of alkali-activated alumino-silicate based, high performance composites In: Advanced structural fiber composites, Ed. Vincenzini, P., *Adv. Sci. Technol.*, **7**, 117 – 124, (1995).

5 Lyon, R.E., Sorathia, U., Balaguru, P., Foden, A., Davidovits, J., Davidovics, M.: Fire response of geopolymer structural composites, *Proceedings of the 1st International conference on composites in infrastructure ICCI*, 1996

6 Lyon, R.E., Balaguru, P.N., Foden, A., Sorathia, U., Davidovits, J., Davidovics, M.: Fire resistant aluminosilicate composites, *Fire. Mater.*, **21**, 67 – 73, (1997).

7 Foden, A., Lyon, R., Balaguru, P.N., Davidovits, J.: High temperature inorganic resin for use in fibre reinforced composites, *Proceedings of the 1st International conference on composites in infrastructure ICCI*, 1996.

8 Foden, A.: Mechanical properties and material characterization of polysialate structural composites, PhD Thesis, Rutgers State University, USA, (1999).

9 Hammell, J., Balaguru, P.N., Lyon, R.: Influence of reinforcement types on the flexural properties of geopolymer composites, *Proceedings of the 43rd International SAMPE Symposium*, 1998.

10 Hammell, J.A., The influence of matrix composition and reinforcement type on the properties of polysialate composites, PhD Thesis, Rutgers State University, USA, (2000).

11 Hammell, J.A., Balaguru, P.N., Lyon, R.E.: Strength retention of fire resistant aluminosilicate-carbon composites under wet-dry conditions, *Compos. Part. B*, **31**, 107 – 111, (2000).

12 He, P., Jia, D., Lin, T., Wang, M., Zhou, Y.: Effects of high-temperature heat treatment on the mechanical properties of unidirectional carbon fibre reinforced geopolymer composites, *Ceram. Int.*, **36**, 1447 – 53, (2010).

13 He, P., Jia, D., Wang, M., Zhou, Y.: Improvement of high-temperature mechanical properties of heat treated C_f/geopolymer composites by sol-SiO_2 impregnation, *J. Eur. Ceram. Soc.*, **30**, 3053 – 61, (2010).

14 He. P., Jia, D., Interface evolution of the C_f/leucite composites derived from C_f/geopolymer composites, *Ceram. Int.*, **39**, 1203 – 08, (2013).

15 Bortnovsky, O., Bezucha, P., Dedecek, J., Sobalik, Z., Vodickova, V., Kroisova, D., Roubicek, P., Urbanova, M.: Properties of phosphorus-containing geopolymer matrix and fibre reinforced composites, In: Mechanical Properties and Performance of Engineering Ceramics and Composites IV, Eds. Singh, D., Kriven, W.M., Salem, J., 283 – 299, (2009).

16 Tran, D.H., Kroisova, D., Louda, P., Bortnovsky, O., Bezucha, P.: Effect of curing temperature on the flexural properties of silica-based geopolymer carbon reinforced composites, *J. Achievements Mater. Manufact. Eng.*, **37**, 492 – 7, (2009).

17 Pernica, D., Reis, P.N.B., Ferreira, J.A.M., Louda, P.: Effect of test conditions on the bending strength of a geopolymer-reinforced composite, *J. Mater. Sci.*, **45**, 744 – 9, (2007).

18 Radford, D.W., Grabher, A., Bridge, J.: Inorganic polymer matrix composite strength related to interface condition, *Materials*, **2**, 2216 – 27, (2009).

19 Lin, T., Jia, D., He, P., Wang, M.: Liang, D.: effects of fiber length on mechanical properties and fracture behaviour of short carbon fiber reinforced geopolymer matrix composites, *Mater. Sci. Eng. A*, **497**, 181 – 5, (2008).

20 Lin, T., Jia, D., Wang, M., He, P., Liang, D.: Effects of fibre content on mechanical properties and fracture behaviour of short carbon fibre reinforced geopolymer matrix composites, *Bull. Mater. Sci.*. **32**, 77 – 81, (2009).

[21] Lin, T., Jia, D., He, P., Wang, M.: In situ crack growth observation and fracture behaviour of short carbon fibre reinforced geopolymer matrix composites, *Mater. Sci. Eng. A*, **527**, 2404 – 7, (2010).

[22] Kriven, W.M., Bell, J.B., Gordon, M.: Microstructure and microchemistry of fully-reacted geopolymers and geopolymer matrix composites, In: advances in ceramic matrix composites IX, *Ceram. Trans.,* **153**, 227 – 50, (2003).

[23] Rill, E., Lowry, D.R., Kriven, W.M.; Properties of basalt fibre reinforced geopolymer composites, *Ceram. Eng. Sci. Proc.*, **31**, 57 – 67, (2010).

[24] Musil, S.S., Kutyla, G.P., Kriven, W.M.: The effect of basalt chopped fibre reinforcement on the mechanical properties of potassium based geopolymer, *Ceram. Eng. Sci. Proc.*, **33**, 31 – 42, (2012).

[25] Li, W., Xu, J.: Mechanical properties of basalt fibre reinforced geopolymeric concrete under impact load, *Mater. Sci. Eng. A*, **505**, 178 – 186, (2009)

[26] Li, W., Xu, J.: Impact characterization of basalt fibre reinforced geopolymeric concrete using a 100 mm-diameter split hopkinson pressure bar, *Mater. Sci. Eng. A*, **513 – 514**, 145 – 15, (2009).

[27]] Dias, D.P., Thaumaturgo, C.: Fracture toughness of geopolymeric concretes reinforced with basalt fibres, *Cement Concrete Comp.*, **27**, 49 – 54, (2005).

[28] [28] Comrie, D.C., Kriven, W.M.: Composite cold ceramic geopolymer in a refractory application, *Ceram. Trans.*, **153**, 211 – 25, (2003).

[29] Defazio, C., Arafa, M.D., Balaguru, P.N.: Functional geopolymer composites for structural ceramic applications, Final Report, Ceram-RU9163, Center for Advanced Infrastructure and Transportation, Rutgers State University, USA, 2006, Available online from: http://cait.rutgers.edu/files/Ceram-RU9163.pdf (accessed: 6.11.2013).

[30] Sun, P., Wu, H.: Transition from brittle to ductile behaviour of fly ash using PVA fibres, *Cement Concrete Comp.*, **30**, 29 – 36, (2008).

[31] Zhang, Y., Sun, W., Li, Z: Impact behaviour and microstructural characteristics of PVA fiber reinforced fly ash-geopolymer boards prepared by extrusion technique, *J. Mater. Sci.*, **41**, 2787 – 2794, (2006).

[32] Zhang, Y., Sun, W., Li, Z., Zhou, X., Eddie, C.: Impact properties of geopolymer based extrudates incorporated with fly ash and PVA short fiber, *Constr. Build. Mater.,* **22**, 370 – 383, (2008).

[33] Zhang, Z, Yao, X., Zhu, H., Hua, S., Chen, Y.: Preparation and mechanical properties of polypropylene fiber reinforced calcined kaolin-fly ash based geopolymer, *J. Cent. South Univ. Technol.*, **16**, 49 – 52, (2009).

[34] Lowry D.R., Kriven W.M.: Effect of high tensile strength polypropylene chopped fibre reinforcements on the mechanical properties of sodium based geopolymer composites, *Ceram. Eng. Sci. Proc.*, **31**, 47 – 56, (2010).

[35] Alzeer, M., MacKenzie, K.J.D.: Synthesis and mechanical properties of new fibre-reinforced composites of inorganic polymers with natural wool fibres, *J. Mater. Sci.*, **47**, 6958 – 65, (2012).

[36] Alzeer, M., MacKenzie, K.J.D.: Synthesis and mechanical properties of novel composites of inorganic polymers (geopolymers) with unidirectional natural flax fibres, *Appl. Clay Sci.*, **75 – 6**, 148 – 152, (2013).

[37] Welter, M.: Unidirectional fibre reinforced geopolymer matrix composites, PhD Thesis, Victoria University of Wellington, New Zealand, (2013).